

Energy Flows in the Jupiter-Io System

¹ Siming Liu¹

¹Key Laboratory of Dark Matter and Space Astronomy, Purple Mountain Observatory, CAS,
Nanjing, China, 210008

Received _____; accepted _____

ABSTRACT

With the laws of mass conservation, momentum conservation and energy conservation, incorporating the processes of neutral gas ionization and ion diffusion, we develop a self-consistent model for the bright ribbon — the most prominent feature in Io’s plasma torus. The model parameters are well constrained by earlier *in situ* observations with the Galileo and Voyager spacecrafts. Our model calculation indicates that the total power dissipated inside the torus is 3.6 times bigger than the total power transported to Jovian ionosphere via Birkeland current. The power dissipation inside the torus is relatively uniform. Most of the power transportation associated with the Birkeland current, however, is localized near the flux tube of Io. With a height-integrated conductivity of 0.15 mho in Jovian ionosphere, consistent with earlier aeronomy models, the model gives a reasonable fit to the recent observations of the FUV Io tail on Jupiter. Extra mass loading near Io is required in the model. This excess of mass injection into the plasma torus may explain the Io-correlated energy source revealed by earlier EUV observations with the Voyager spacecrafts. Further investigation of the model implications is warranted.

Subject headings: Jupiter—Jovian satellites—Orbital and rotational dynamics—Magnetosphere/ionosphere interactions—magnetic fields

1. Introduction

The coupling between magnetosphere and ionosphere in solar planets reveals many important physical processes, which may have significant implications on distant astrophysical systems [Mauk, Anderson and Thorne, 2002]. Since first detected in 1964 [Bigg 1964], the Io correlated Jovian decametric bursts have been well studied [Goldreich and Lynden-Bell 1969; Riihimaa 1968; Imai, Wang and Carr 1997]. The implied interaction between Jupiter and Io has been attracting attention in the community for more than two decades [Dessler 1983; Belcher 1987].

Pioneer 11 first detected a plasma concentration near Io [Fillius, McIlwain and Mogro-Campero 1975], which was later revealed by Voyager 1 as a plasma torus [Broadfoot et al. 1979]. The powerful EUV emission from this Io’s plasma torus ($\sim 3 \times 10^{12}$ W) has posed a theoretical challenge since it was confirmed by Voyager 2 [Sandel et al. 1979]. Several models have been developed to account for this, among which are the unipolar inductor model [Goldreich and Lynden-Bell 1969, Belcher 1987], the Alfvén wing theory [Drell, Foley and Ruderman 1965; Neubauer 1980] and the model with an extended neutral cloud distributed in the torus [Brown and Ip 1981; Trauger 1984], with the last one being favored both theoretically [Barbosa, Coroniti and Eviatar 1983; Barbosa 1994; Shemansky 1980] and observationally [Smyth and Shemansky 1983; Skinner and Durrance 1986]. Although all the models achieve in explaining certain observations, a global picture of the Jupiter-Io coupling system, which unifies these models, does not exist.

Significant progresses were made in recently years with the detection of Io’s footprint on Jovian ionosphere both at IR with the NASA IRTF [Connerney et al. 1993; Satoh and Connerney 1999] and at UV with the Hubble Space Telescope (HST) [Clarke et al. 1996]. This is especially the case for the newly reported downstream emission of the Io’s footprint [Clarke et al. 2002] since it indicates strong coupling between Jupiter’s ionosphere and Io’s plasma torus over an extend region [Hill and Vasyliúnas 2002; Gérard et al. 2002]. Now observations exist on both ends of this coupling system. Combining the recent HST observations on the Io’s footprint with the Galileo spacecraft’s *in situ* measurements [Frank et al. 1996; Kivelson et al. 1996; Gurnett et al. 1996], we develop a self-consistent model for one of the key features in the Io’s plasma torus—the bright

ribbon [Trauger 1984; Dessler and Sandel 1993; Schneider and Trauger 1995; Volwerk et al. 1997].

Our basic model assumption is that, led by Io, the extended neutral cloud is concentrated within a narrow region of a few Io’s radii. Then a self-consistent hydrodynamical model is developed for such a cloud with ionization and plasma diffusion processes parameterized. The ionization of this neutral gas will not only energize the plasma around it, which eventually lead to the formation of the bright ribbon feature detected in the torus, but also induce significant Birkeland currents which close in the northern and southern Jovian ionospheres, producing the Io’s footprint and its downstream emission. Thus correlation is expected between emissions from the ribbon and that from its footprint. In the paper, we mainly study the energy flows in the system. Our model calculation indicates that the energy transportation to Jovian ionosphere via Birkeland current, which is localized near Io’s flux tube, is comparable to the energy dissipation in the plasma torus, which is relatively uniform along the ribbon. Future coordinated observations will be able to test the model.

In § 2, we briefly discuss the basic ideas for introducing such a model and develop full dynamical equations for the ribbon. The observational constraints on the model parameters are discussed in § 3. We then show that there is a very simple analytical solution to the dynamical equations. In § 4, we calculate the model predicted energy flows and compare them with observations. Our conclusions are drawn in § 5.

2. Model Description and Basic Equations

There is much observational evidence for the existence of an extended neutral cloud in the Io’s plasma torus [see e.g. Smyth and Shemansky 1983; Skinner and Durrance 1986]. Theoretically, Shemansky [1980] first pointed out that the mass loading around Io is so insufficient that the heating of the plasma induced by it cannot balance the cooling due to EUV emission from the plasma torus. This conclusion was later confirmed by the Galileo *in situ* measurement [Bagenal 1997]. Russell and Huddleston [2000] recently showed that a small mass loading rate near Io

is also consistent with observations of the Jupiter-Io system made over the past three decades. This small mass loading rate near Io then suggests an extended mass loading region, which may be associated with the extended neutral cloud observed.

A narrow ribbon in the Io’s plasma torus was first reported by Trauger [1984] with Earth-based optical observations. Dessler and Sandel [1993] later showed that the strong EUV emission from the torus detected by the Voyagers is confined within a region less than $9 R_I$ in width, where $R_I = 1.8 \times 10^6$ m is the radius of Io, consistent with Galileo observations which reveal dramatic changes in the plasma’s property while Galileo flying through the narrow wake of Io ($\sim 6 R_I$) [Frank et al. 1996; Kivelson et al. 1996; Gurnett et al. 1996]. The recent high-quality images of [S II] 6731 Å emissions from S^+ , on the other hand, show this plasma feature in unprecedented detail [Schneider and Trauger 1995].

Because we are mostly interested in its time-averaged properties, the ribbon can then be approximated as in a steady state. We will assume that the narrow ribbon is surrounded by a background plasma and the plasma and neutral gas distributions inside the ribbon only depend on their azimuthal coordinate. By neglecting the variations of the gas and plasma properties in the radial and vertical directions inside the ribbon, we reduce the study to an one dimensional problem. As the first step of such an investigation, these approximations are good enough to address the relevant energy transportation processes. However the detailed gas and plasma distributions will control the corresponding diffusion and ionization processes, which are crucial for a self-consistent hydrodynamical model. In the following discussion, we will parameterize these processes in accord with these approximations.

We will develop the model in Io’s rest frame. Then the mass conservation law is given by:

$$\frac{d\rho}{dt} = \frac{\partial \rho}{\partial t} + \nabla(\rho \mathbf{v}), \quad (1)$$

where ρ is the mass density of the ions inside the ribbon and $\mathbf{v} = v \mathbf{e}_\phi$ is the plasma’s velocity. The neutral gas is roughly in a Keplerian orbit. Thus its velocity in Io’s rest frame is zero. Then

we have

$$(\rho v)' = \frac{\rho_n}{\tau_n} - \frac{\rho - \rho_b}{\tau_i}, \quad (2)$$

where ρ_n is the neutral gas mass density, which is zero outside the ribbon, ρ_b is the background ion density, τ_n is the mean lifetime of the neutral gas, which characterizes the ionization processes and τ_i is the diffusion time scale of the ions. A prime here denotes derivative with respect to the azimuthal coordinate. In obtaining equation (2), we have assumed that the background ions only have the effect of suppressing the diffusive loss of ions from the ribbon.

From the momentum conservation equation

$$\frac{d\rho\mathbf{v}}{dt} = \frac{\partial\rho\mathbf{v}}{\partial t} + \nabla(\rho\mathbf{v}\mathbf{v}), \quad (3)$$

we have

$$jB - \frac{\rho - \rho_b}{\tau_i}v = v(\rho v)' + \rho vv', \quad (4)$$

where j is the current density and B is the strength of the magnetic field. The first term on the LHS of equation (4) comes from the current acceleration by the magnetic field. The second term is associated with the diffusive loss of ions from the ribbon. Combining this equation with equation (2), we get

$$jB = \frac{\rho_n}{\tau_n}v + \rho vv', \quad (5)$$

which says that the current acceleration provides the momentum to speed up the ion newly produced via neutral gas ionization, which corresponds to the first term on the RHS, and the momentum to accelerate the plasma flow as indicated by the second term on the RHS.

The energy conservation law is given by

$$\frac{d\rho\epsilon}{dt} = \frac{\partial\rho\epsilon}{\partial t} + \nabla(\rho\mathbf{v}\epsilon), \quad (6)$$

where $\epsilon = v^2/2 + \epsilon_{th}$ is the plasma energy density per unit mass and ϵ_{th} is the plasma's thermal energy density per unit mass. From this, we have

$$jE - \Lambda - \frac{\rho - \rho_b}{\tau_i} \left(v^2/2 + \epsilon_{th} \right) = (\rho v)'(v^2/2 + \epsilon_{th}) + \rho v^2 v' + \rho v \epsilon'_{th}, \quad (7)$$

where $E = vB$ is the electric field, Λ is the cooling rate due to line emission. Multiplying equation (5) with v , we have

$$jE = \frac{\rho_n}{\tau_n}v^2 + \rho v^2 v'. \quad (8)$$

Combining this equation with equation (7), one then gets

$$\Lambda = \frac{\rho_n}{\tau_n} \left(v^2/2 - \epsilon_{th} \right) - \rho v \epsilon'_{th}. \quad (9)$$

This equation shows the energy balance between the cooling due to line emission and the heating introduced by the injection of new plasma produced through neutral cloud ionization, corresponding to the first term on the RHS, and energy advection which corresponds to the second term on the RHS.

To calculate the power carried by Birkeland current, which includes the power dissipated in the Jovian ionosphere and that consumed in the electron accelerating double layers [Mauk et al. 2002], we note that the e.m.f. per unit length produced by the plasma inside the ribbon equals Bv_0 , where $v_0 = 57 \text{ km s}^{-1}$ is the rigid corotation velocity at Io's orbit. Multiplying equation (5) with $(v_0 - v)$, we have

$$jE_J = \frac{\rho_n}{\tau_n}v(v_0 - v) + \rho v v'(v_0 - v), \quad (10)$$

where $E_J = B(v_0 - v)$ is the electric field in Jupiter's co-rotation frame. Then the LHS gives the power of the Birkeland current. The first term on the RHS comes from the pickup current and the second term is associated with the acceleration current.

Equation (5) can be written as

$$J = \frac{\eta_n}{\tau_n}v + \eta v v', \quad (11)$$

where $J = \int dz j$ is the height-integrated current density, $\eta_n = \int dz(\rho_n/B)$ and $\eta = \int dz(\rho/B)$ are the neutral gas content and plasma content per unit magnetic flux inside the ribbon respectively. This current closes in the Jovian ionosphere. Then the current continuity equation can be written as [Hill 2002]

$$J = 2J_\theta L^{-3/2}, \quad (12)$$

where

$$J_\theta = \Sigma E_\theta \quad (13)$$

is the height-integrated Peterson current, Σ is the height-integrated conductivity of Jovian ionosphere [Strobel et al. 1983], E_θ is the strength of the electric field in Jovian ionosphere and $L = 1/\sin^2 \theta$. If we neglect the potential drop across the double layers in the Birkeland circuit, we have

$$E_\theta = -E_J(dL/d\theta) = 2E_J L^{3/2}. \quad (14)$$

Then from equations (11), (12), (13), (14) and (2), we have the basic equations for the ribbon:

$$4\Sigma B(v_0 - v) = \frac{\eta_n}{\tau_n}v + \eta v v', \quad (15)$$

$$\frac{\eta_n}{\tau_n} - \frac{\eta - \eta_b}{\tau_i} = (\eta v)', \quad (16)$$

where $\eta_b = \int dz(\rho_b/B)$ is the plasma content per unit magnetic flux of the background within which the ribbon embedded. Then if we neglect the neutral gas injection and plasma diffusion, i.e. let $\eta_n/\tau_n = (\eta - \eta_b)/\tau_i = 0$, we have the results reported by Hill [2002]. Note in Hill's paper, he assumed that η is a constant, which is actually a very crude treatment of the plasma diffusion processes and the mass conservation law. Our equations are accurate with the corresponding physical processes parameterized. On the other hand, if we neglect the acceleration current, we have the results given by Hill and Pontius [1998] and by Pontius and Hill [1982].

3. Model Parameters and an Analytical Solution

In equations (15) and (16), η_n/τ_n depends on the mechanism through which the neutral gas is picked up from Io and gets ionized, and η_b depends on how the plasma diffuses away from the torus. Because both processes are not well understood, we will leave η_n/τ_n , η_b as input functions. B is measured by Kivelson et al. [1996] with the magnetometer on Galileo: $B \sim 1400$ nT. Σ is given by aeronomy models [e.g., Strobel and Atreya, 1983]. We will adopt a fiducial value of 0.1 mho. For given η_n and η_b , τ_i can be fixed by the steady state condition (we will address this in detail in the following discussion) when we solve the equations for v and η . Then with

the thermal properties of the plasma determined with models of the corresponding microscopic processes [Barbosa, Coroniti and Eviatar 1983], we can calculate the model predicated emissions from the ribbon, which can be compared with observations directly. At the same time, the power of the Birkeland current can be associated with observations on the Io’s footprints on Jovian ionosphere [Clarke et al 2002]. Strong correlation between emissions from the torus and that from Io’s footprints is expected.

To solve the equations numerically, it is convenient to put the equations in a dimensionless form. We define

$$v(\phi) = f(\phi)v_0, \quad (17)$$

$$\frac{\eta_n}{\tau_n} = \lambda_0 \Lambda(\phi), \quad (18)$$

$$\eta = \lambda_0 \tau_0 g(\phi), \quad (19)$$

$$\eta_b = \lambda_0 \tau_0 g_b(\phi), \quad (20)$$

where

$$\tau_0 = \frac{LR_J}{v_0} = 7.3 \times 10^3 \text{sec} \left(\frac{R_J}{7.1 \times 10^7 \text{m}} \right) \left(\frac{L}{5.9} \right) \left(\frac{5.7 \times 10^4 \text{m sec}^{-1}}{v_0} \right) \quad (21)$$

gives the characteristic dynamical time scale. λ_0 is defined as

$$\lambda_0 = \frac{\dot{M}}{B 2\pi L R_J w}, \quad (22)$$

where \dot{M} is the total mass injection rate throughout the ribbon, $L = 5.9$ is orbital radius of the torus [Broadfoot et al. 1979], $R_J = 7.1 \times 10^7$ m is Jupiter’s radius, w is the width of the ribbon. We will assume that the ribbon has a width of $6 R_I$. Observations [[Trauger 1984; Dessler and Sandel 1993; Schneider and Trauger 1995] indicate that the height of the narrow bright feature in Io’s plasma torus is $\sim R_J$, which is much larger than the width of the ribbon. This is because the diffusion of ions is not isotropic in the plasma torus due to the existence of the strong magnetic field, which is roughly perpendicular to the plasma’s orbital plane. Such an anisotropy will make the plasma spread out in the direction parallel to the magnetic field line. And the deviation of the magnetic field line from the vertical direction also enhances this effect when we have new ions

produced via neutral gas ionization as is the case in our model. Because the observed feature is associated with the ion distribution directly, we would expect that the emission region be more extended in the vertical direction than in the radial direction. However, the diffusion of neutral gas is almost isotropic. So we can assume that the cross section of the ribbon is a square.

There are several independent estimates of the mass injection rate into the torus. The UVS observation shows the total power of the UV emission from the torus is no less than 2.5×10^{12} W [Sandel et al., 1979], implying a mass loading rate $\dot{M} > 1.6 \times 10^3 \text{ kg sec}^{-1}$ [Siscoe and Chen, 1977]. Dessler [1980] show that $\dot{M} > 10^3 \text{ kg sec}^{-1}$ based on the energy supply to the Jovian magnetosphere from Jupiter’s rotation. The plasma production via ionization of the neutral gas from Io in the magnetosphere will induce a slip of the plasma relative to corotation as the plasma flows outwards and angular momentum is transported from Jupiter out to the plasma flow [Hill 1979]. Voyager 1 plasma observations [Bridge et al. 1979] indicate: $\dot{M} \sim 1.7 \times 10^3 (\Sigma/0.1\text{mho}) \text{ kg sec}^{-1}$ [Hill, 1980]. So $2.0 \times 10^3 \text{ kg sec}^{-1}$ is a reasonable fiducial mass injection rate.

Then we have

$$\lambda_0 = 5.0 \times 10^{-8} \left(\frac{\dot{M}}{2 \times 10^3 \text{kg s}^{-1}} \right) \left(\frac{1400 \text{nT}}{B} \right) \left(\frac{5.9}{L} \right) \left(\frac{7.1 \times 10^7 \text{m}}{R_J} \right) \left(\frac{1.1 \times 10^7 \text{m}}{w} \right) \text{kg (sTm}^2)^{-1}. \quad (23)$$

Equations (15) and (16) then can be written as:

$$\sigma(1 - f) = \Lambda f + g f \frac{df}{d\phi}, \quad (24)$$

$$\Lambda - \alpha(g - g_b) = \frac{d(gf)}{d\phi}, \quad (25)$$

where $\alpha = \tau_0/\tau_i$ and

$$\sigma = \frac{4\Sigma B}{\lambda_0} = 11.3 \left(\frac{\Sigma}{0.1\text{mho}} \right) \left(\frac{B}{1400 \text{nT}} \right) \left(\frac{5.0 \times 10^{-8} \text{kg (sTm}^2)^{-1}}{\lambda_0} \right).$$

A self-consistent steady state solution is also subject to the following constraints:

$$\int d\phi R_J L w \frac{\eta_n}{\tau_n} = \frac{\dot{M}}{B} \iff \int d\phi \Lambda = 2\pi, \quad (26)$$

$$\int d\phi R_J L w \left(\frac{\eta_n}{\tau_n} - \frac{\eta - \eta_b}{\tau_i} \right) = 0 \iff \int d\phi [\Lambda - \alpha(g - g_b)] = 0. \quad (27)$$

The first constraint sets the normalization condition for Λ . To get the second constraint, we have assumed that the flux of the plasma inside the ribbon satisfies the periodic boundary condition. However, other physical properties of the plasma don't need to be continuous across Io because shocks will be produced there. For given neutral cloud distribution in the torus, $\Lambda(\phi)$, satisfying condition (26), background ion distribution g_b and boundary conditions $f(0)$ and $g(0)$, it is obvious that not all the solutions of equations (24) and (25) satisfy condition (27). Only certain value of α (eigen value) can make condition (27) satisfied. For arbitrary input functions $\Lambda(\phi)$ and g_b , we must choose an α to get a solution, then we check on condition (27) and adjust α until it is satisfied. The calculation is quite complicated.

Fortunately, in the case that $\Lambda - \alpha(g - g_b) = 0$ everywhere and g_b is a constant, which we call local equilibrium in a smooth background, we have the following solution:

$$f = \frac{\sigma - c_1\alpha}{\sigma - \alpha g_b} \left(1 - c_2 e^{-(\sigma - \alpha g_b)\phi/c_1} \right), \quad (28)$$

$$g = c_1/f, \quad (29)$$

$$\Lambda = \alpha(g - g_b), \quad (30)$$

where $c_1 = gf$, $c_2 = 1 - (\sigma - \alpha g_b)f(0)/(\sigma - \alpha c_1)$ can be fixed with the boundary conditions $f(0)$ and $g(0)$. Galileo observation shows that the averaged mass flux in Io's wake is about $\langle \rho v \rangle \sim 1.4 \times 10^{-11} \text{ kg sec}^{-1} \text{ m}^{-2}$, where we have used a background speed of $5.3 \times 10^4 \text{ m sec}^{-1}$ [Bagenal 1997]. We also assumed a mean ion mass of 24 amu [Hill 2002]. From this we have

$$\begin{aligned} c_1 &= \frac{H \langle \rho v \rangle}{v_0 \tau_0 \lambda_0 B} \\ &= 5.2 \left(\frac{5.7 \times 10^4 \text{ m s}^{-1}}{v_0} \right) \left(\frac{7.3 \times 10^3 \text{ s}}{\tau_0} \right) \left(\frac{5.0 \times 10^{-8} \text{ kg (sTm}^2)^{-1}}{\lambda_0} \right) \\ &\quad \left(\frac{1400 \text{ nT}}{B} \right) \left(\frac{H}{w} \right) \left(\frac{w}{6R_I} \right) \left(\frac{R_I}{1.8 \times 10^6 \text{ m}} \right) \left(\frac{\langle \rho v \rangle}{1.4 \times 10^{-11} \text{ kg s}^{-1} \text{ m}^{-2}} \right). \end{aligned} \quad (31)$$

Galileo observations also reveal a sharp increase of electron number density and decrease in the flow velocity in Io's wake. And the background mass flux is $\langle \rho v \rangle_b \sim 8.0 \times 10^{-12} \text{ kg sec}^{-1} \text{ m}^{-2}$. We will adopt a value of $3.0 \times 10^4 \text{ m sec}^{-1}$ as a characteristic averaged initial velocity of the flow inside the ribbon. Then the initial mean mass density of the plasma is $4.8 \times 10^{-16} \text{ kg m}^{-3}$,

corresponding to an ion number density of 12000 cm^{-3} . Then we have

$$g_b = 3.2 \left(\frac{5.3 \times 10^4 \text{ m s}^{-1}}{v_b} \right) \left(\frac{7.3 \times 10^3 \text{ s}}{\tau_0} \right) \left(\frac{5.0 \times 10^{-8} \text{ kg (sTm}^2)^{-1}}{\lambda_0} \right) \left(\frac{1400 \text{ nT}}{B} \right) \left(\frac{H}{w} \right) \left(\frac{w}{6R_I} \right) \left(\frac{R_I}{1.8 \times 10^6 \text{ m}} \right) \left(\frac{< \rho v >_b}{8.0 \times 10^{-12} \text{ kg s}^{-1} \text{ m}^{-2}} \right), \quad (32)$$

$$c_2 = 1 - 0.53 \left[\frac{v_i}{v_o} \right] \left(\frac{11.3[\sigma/11.3] - 3.2\alpha[g_b/3.2]}{11.3[\sigma/11.3] - 5.2\alpha[c_1/5.2]} \right). \quad (33)$$

From the normalization condition (26) we have:

$$\frac{\alpha c_1^2}{\sigma - c_1 \alpha} \left[\frac{2\pi(\sigma - \alpha g_b)}{c_1} + \ln(1 - c_2 e^{-2\pi(\sigma - \alpha g_b)/c_1}) - \ln(1 - c_2) \right] = 2\pi(1 + g_b \alpha). \quad (34)$$

Solving this equation for α , we get an analytical solution for the structure of the ribbon.

4. Model Fit to Observations

The power per unit magnetic flux carried by the Birkeland current is given by

$$P_B = \int dz \frac{E_J j}{B} = \lambda_0 v_0^2 (1 - f) f [\Lambda + g(df/d\phi)]. \quad (35)$$

The corresponding dissipation inside the torus is given by

$$\begin{aligned} P_t &= \int dz \left(\frac{\rho_n}{2\tau_n B} v^2 + \frac{\rho - \rho_b}{2\tau_i B} (v_b - v)^2 \right) \\ &= 0.5 \lambda_0 v_0^2 [\Lambda f^2 + \alpha(g - g_b)(v_b/v_0 - f)^2]. \end{aligned} \quad (36)$$

These powers can be compared with observations with appropriate models which can predict the observed emission from the Jupiter-Io system. Fitting observations of the FUV Io tail on Jupiter [Gérard et al. 2002], we find

$$\Sigma = 0.15 \text{ mho}, \quad (37)$$

$$\sigma = 17. \quad (38)$$

Then solving equations (33) and (34), one has

$$\alpha = 0.41, \quad (39)$$

$$c_2 = 0.44. \quad (40)$$

So we have the structure of the ribbon:

$$f = 0.95 - 0.42e^{-3.0\phi}, \quad (41)$$

$$g = 5.2/(0.95 - 0.42e^{-3.0\phi}), \quad (42)$$

$$\Lambda = 2.1/(0.95 - 0.42e^{-3.0\phi}) - 1.3, \quad (43)$$

$$P_B = 160 (0.05 + 0.42e^{-3.0\phi}) (0.87 + 7.1e^{-3.0\phi}) \left(\frac{\lambda_0}{5.0 \times 10^{-8}} \right) \left(\frac{v_0}{5.7 \times 10^4 \text{ m s}^{-1}} \right)^2 \text{ W m}^{-2} \text{ T}^{-1}, \quad (44)$$

$$P_t = 81 \left(\frac{2.1}{0.95 - 0.42e^{-3.0\phi}} - 1.3 \right) (0.90 - 0.80e^{-3.0\phi} + 0.35e^{-6.0\phi}) \left(\frac{\lambda_0}{5.0 \times 10^{-8}} \right) \left(\frac{v_0}{5.7 \times 10^4 \text{ m s}^{-1}} \right)^2 \text{ W m}^{-2} \text{ T}^{-1}. \quad (45)$$

In figure 1 we give the normalized power distributions in the azimuthal direction. The model gives a reasonable fit to observations of the FUV Io tail on Jupiter. Figure 2 shows the integrated power distributions. The integrations start at Io. From this we see that most of the power associated with the Birkeland current is localized around Io. However, the power dissipation in the torus is quite uniform. The model then fails to explain the Io phase effect which says that about 20% of the EUV power from the Io's plasma torus is correlated with Io [Sandel & Broadfoot 1982b]. This is not a surprise given our crude treatment of the boundary conditions near Io. Galileo *in situ* observations show that the power supplied to the torus near Io accounts for 15% to 28% of the total EUV power from the torus [Bagenal 1997], suggesting that Io phase effect is associated with the processes near Io. Investigation of these processes is beyond the scope of this paper. A global self-consistent picture of the Jupiter-Io system should incorporate these processes with the model we developed here for the ribbon.

We also note that the total power dissipated in the torus is $2.7 \times 10^{12} \text{ W}$, which is consistent with the EUV observations of emission from the torus. The power associated with the Birkeland current is $1.1 \times 10^{12} \text{ W}$ which, when combined with the observed FUV power from Io's footprint, implies a FUV radiation efficiency of $\sim 10\%$. This total power supply to Jovian ionosphere via Birkeland current sets a very strict constraint on the excitation mechanism of the FUV Io tail. When combining with an auroral atmosphere model, one can infer an model predicted H_3^+

brightness at Io’s footprint, which can be compared with the corresponding observations. The total power supplied to the torus via ionization of the neutral cloud in the ribbon is given by

$$P = \frac{1}{2} \dot{M} v_b^2 = 3.2 \times 10^{12} \text{ W} \left(\frac{\dot{M}}{2 \times 10^3 \text{ kg s}^{-1}} \right) \left(\frac{v_b}{5.3 \times 10^4 \text{ m s}^{-1}} \right)^2, \quad (46)$$

which is smaller than the sum of the power dissipated in the torus and that associated with the Birkeland current. The power excess comes from the mass loading near Io, which breaks the periodic conditions for the ribbon. So there is a net energy flux from the ends of the ribbon, where Io locates.

In figure 3, we show the current distribution J in the azimuthal direction, where

$$J = 1.2 \times 10^6 (0.87 + 7.1e^{-3.0\phi}) \text{ Am rad}^{-1}, \quad (47)$$

and the integrated current. The current near Io is $\sim 4 \times 10^6$ Ampere, which is consistent with Voyager 1 *in situ* observations [Belcher 1987]. The total current across the ribbon is 9.6×10^6 Ampere. Because the newly produced ion via ionization of the neutral cloud gains momentum through the current, we can estimate the total current across ribbon from the mass injection rate in the torus:

$$I = \frac{\dot{M} v_b}{w B} = 7.0 \times 10^6 \text{ Am} \left(\frac{\dot{M}}{2 \times 10^3 \text{ kg s}^{-1}} \right) \left(\frac{v_b}{5.3 \times 10^4 \text{ m s}^{-1}} \right) \left(\frac{1400 \text{ nT}}{B} \right) \left(\frac{1.1 \times 10^7 \text{ m}}{w} \right). \quad (48)$$

The fact that this current is smaller than the value from our numerical calculation also suggests local excess of mass injection near Io, which requires extra current to accelerate the ions in the ribbon to the velocity of the background plasma.

5. Conclusions

In this paper, we develop a self-consistent model for the bright ribbon in Io’s plasma torus. Most of the model parameters were determined theoretically or via observations. Thus the model is well constrained. To compare with observations of the FUV Io tail on Jupiter, we gave the simplest analytical solution of the equations, which control the structure of the ribbon. The model

predicts a neutral cloud ionization rate as:

$$\frac{\rho_n}{\tau_n} = 6.4 \times 10^{-27} \text{ kg cm}^{-3} \text{ s}^{-1} \left(\frac{2.1}{0.95 - 0.42e^{-3.0\phi}} - 1.3 \right), \quad (49)$$

which can be combined with a model detailing the ionization processes of the neutral cloud to make predictions on observations in the optical band [Smyth and Shemansky 1983].

The model also requires an ion distribution of

$$n_i = \frac{6400}{0.95 - 0.42e^{-3.0\phi}} \text{ cm}^{-3}, \quad (50)$$

inside the ribbon. This number density is higher than the canonical value of 2000 cm^{-3} by more than a factor of 3. Although this high number density implies a relatively larger cooling rate, the density is not high enough to explain the short cooling time reported by Volwerk et al. [1997]. However, we noticed that the lack of correlation between the brightnesses of the two ansae can also be explained as due to some plasma processes, such as plasma waves et al. These processes can dump a local enhancement of energy density with the corresponding time scales. For example, the Alfvén velocity inside the ribbon is more than two times bigger than the co-rotation velocity at Io. The corresponding time scale is more than two times smaller than the corresponding dynamical time scale which is enough to explain the observed the lack of correlation. Further investigation of its implication on the EUV emission processes is warranted [Barbosa, Coroniti, and Eviatar 1983a].

Acknowledgments

REFERENCES

- Bagenal, F., The ionization source near Io from Galileo wake data, *Geophys. Res. Lett.* *24*, 2111, 1997.
- Barbosa, D. D., Neutral cloud theory of the Jovian nebula: Anomalous ionization effect of superthermal electrons, *Astrophys. J.* *430*, 376, 1994.
- Barbosa, D. D., F. V. Coroniti, and A. Eviatar, Coulomb thermal properties and stability of the Io plasma torus, *Astrophys. J.* *274*, 429, 1983.
- Barbosa, D. D., and M. G. Kivelson, Dawn-dusk electric field asymmetry of the Io plasma torus, *Geophys. Res. Lett.*, *10*, 210, 1983.
- Barbosa, D. D., Comment on the paper "System III variations in apparent distance of Io plasma torus from Jupiter, *Geophys. Res. Lett.*, *20*, 2487, 1993.
- Belcher, J. W., The Jupiter-Io connection: An Alfvén engine in space, *Science*, *238*, 170, 1987.
- Bigg, E. K., Influence of the satellite Io on Jupiter's decametric emission, *Nature*, *203*, 1008, 1964.
- Bridge, H. S., et al., Plasma observations near Jupiter: Initial results from Voyager 1, *Science*, *204*, 987, 1979.
- Broadfoot, A. L., et al., Extreme ultraviolet observations from Voyager 1 encounter with Jupiter, *Science*, *204*, 979, 1979.
- Brown, R. A., and W.-H. Ip, Atomic clouds as distributed sources for the Io plasma torus, *Science*, *213*, 1493, 1981.
- Clarke, J. T., et al., Far-ultraviolet imaging of Jupiter's aurora and the Io "footprint", *Science*, *274*, 404, 1996.
- Clarke, J. T., et al., Ultraviolet emissions from the magnetic footprints of Io, Ganymede and Europa on Jupiter, *Nature*, *415*, 997, 2002.

- Connerney, J. E. P., R. Barton, T. Satoh, and T. Owen, Imaging of excited H_3^+ at the foot of the Io flux tube in Jupiter’s atmosphere, *Science*, *262*, 1035, 1993.
- Dessler, A. J., Mass-injection rate from Io into the Io plasma torus, *Icarus*, *44*, 291, 1980.
- Dessler, A. J., Physics of the Jovian magnetosphere, Cambridge University Press, Cambridge, 1983.
- Dessler, A. J., and B. R. Sandel, System III variations in apparent distance of Io plasma torus from Jupiter, *Geophys. Res. Lett.*, *19*, 2099, 1992.
- Dessler, A. J., and B. R. Sandel, Reply to comment by D. D. Barbosa, *Geophys. Res. Lett.*, *20*, 2489, 1993.
- Drell, S. D., H. M. Foley, and M. A. Ruderman, Drag and propulsion of large satellites in the ionosphere: An Alfvén propulsion engine in space, *J. Geophys. Res.*, *70*, 3131, 1965.
- Fillius, R. W., C. E. McIlwain, and A. Mogro-Campero, Radiation belts of Jupiter: A second look, *Science*, *188*, 465, 1975.
- Frank, L. A., W. R. Paterson, K. L. Ackerson, V. M. Vasyliunas, F. V. Coroniti, and S. J. Bolton, Plasma observations at Io with the Galileo spacecraft, *Science*, *274*, 394, 1996.
- Gérard, J.-C., J. Gustin, D. Grodent, P. Delamere, and J. T. Clarke, The excitation of the FUV Io tail on Jupiter: characterization of the electron precipitation, Submitted to *J. Geophys. Res.* 2002.
- Goldreich, P., and D. Lynden-Bell, Io, A Jovian unipolar inductor, *Astrophys. J.*, *156*, 59, 1969.
- Gurnett, D. A., W. S. Kurth, A. Roux, S. J. Bolton, and C. F. Kennel, Galileo plasma wave observations in the Io plasma torus and near Io, *Science*, *274*, 391, 1996.
- Hill, T. W., Inertial limit on corotation, *J. Geophys. Res.*, *84*, 6554, 1979.
- Hill, T. W., Corotation lag in Jupiter’s magnetosphere: Comparison of observation and theory, *Science*, *207*, 301, 1980.

- Hill, T. W., D. H. Pontius Jr., Plasma injection near Io, *J. Geophys. Res.*, *103*, 19879, 1998.
- Hill, T. W., V. M. Vasyliunas, Jovian auroral signature of Io’s corotational wake, Submitted to *J. Geophys. Res.* 2002.
- Imai, K., L. Wang, and T. D. Carr, Modeling Jupiter’s decametric modulation lanes, *J. Geophys. Res.*, *102*, 7127, 1997.
- Ip, W.-H., and C. K. Goertz, An interpretation of the dawn-dusk asymmetry of UV emission from the Io plasma torus, *Nature*, *302*, 232, 1983.
- Kivelson, M. G., et al., Io’s Interaction with the plasma torus: Galileo magnetometer report, *Science*, *274*, 396, 1996.
- Mauk, B. H., B. J. Anderson, and R. M. Thorne, Magnetosphere-ionosphere coupling at Earth, Jupiter, and beyond, *Comparative Aeronomy: AGU Geophys. Mono.*, In press.
- Neubauer, F. M., Nonlinear standing Alfvén wave current system at Io: Theory, *J. Geophys. Res.*, *85*, 1171, 1980.
- Pontius, D. H., Jr., The Io current wing, Submitted to *J. Geophys. Res.*, 2002.
- Pontius, D. H., Jr., and T. W. Hill, Departure from corotation of the Io plasma torus: Local plasma production, *Geophys. Res. Lett.* *9*, 1321-1324, 1982.
- Riihimaa, J. J., Structured events in the dynamic spectra of Jupiter’s decametric radio emission, *Astron. J.*, *73*, 265, 1968.
- Roesler, F. L., et al., Far-ultraviolet imaging spectroscopy of Io’s atmosphere with HST/STIS, *Science*, *283*, 353, 1999.
- Russell, C.T., and D. E. Huddleston, The unipolar inductor myth: Mass addition or motional electric field as the source of field aligned currents at Io, *Adv. Space Res.*, *26*, 1665, 2000.
- Sandel, B. R., and A. L. Broadfoot, Io’s hot plasma torus — A synoptic view from Voyager, *J. Geophys. Res.*, *87*, 212, 1982a.

- Sandel, B. R., and A. L. Broadfoot, Discover of an Io-correlated energy source for Io’s hot plasma torus, *J. Geophys. Res.*, *87*, 2231, 1982b.
- Sandel, B. R., et al., Extreme ultraviolet observations from Voyager 2 encounter with Jupiter, *Science*, *206*, 962, 1979.
- Satoh, T., and J. E. P. Connerney, Jupiter’s H_3^+ emissions viewed in corrected jovimagnetic coordinates, *Icarus*, *141*, 236, 1999.
- Schneider, N. M., and J. T. Trauger, The Structure of the Io Torus, *ApJ*, *450*, 450, 1995.
- Siscoe, G. L., and C. K. Chen, Io - A source for Jupiter’s inner plasmasphere, *Icarus*, *31*, 1, 1977.
- Skinner, T. E., and S. T. Durrance, Neutral oxygen and sulfur densities in the Io torus, *Astrophys. J.*, *310*, 966, 1986.
- Smyth, W. H., and D. E. Shemansky, Escape and ionization of atomic oxygen from Io, *ApJ*, *271*, 865, 1983.
- Strobel, D. F., and S. K. Atreya, Ionosphere, in *Physics of the Jovian magnetosphere*, edited by A. J. Dessler, p. 66, Cambridge University Press, Cambridge, 1983.
- Trauger, J. T., The Jovian nebula: A post-Voyager perspective, *Science*, *226*, 337, 1984.
- Volwerk, M., M. E. Brown, A. J. Dessler, and B. R. Sandel, Evidence for short cooling time in the Io plasma torus, *Geophys. Res. Lett.*, *24*, 1147, 1997.
- Williams D. J., et al., Electron beams and ion composition measured at Io and in its torus, *Science*, *274*, 401, 1996.

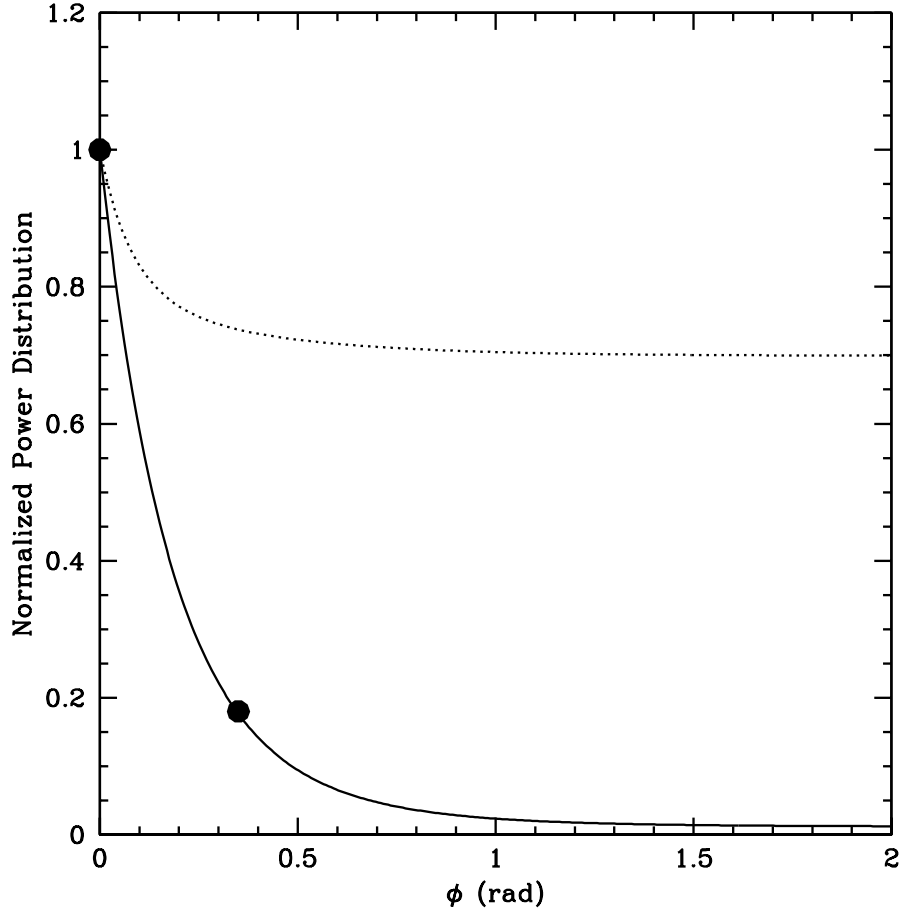


Fig. 1.— Normalized power distributions in the azimuthal direction. The solid line gives the power distribution associated with the Birkeland current (P_B), which should be compared with observations of the downstream emission of Io’s footprint on Jupiter. The dotted line is for the power dissipation in the torus (P_t). Both curves are normalized to their initial values which are $3.9 \times 10^{12} \text{ W rad}^{-1}$, and $6.1 \times 10^{11} \text{ W rad}^{-1}$ respectively. The dots correspond to the data inferred from observations of the FUV Io tail on Jupiter [Gérard et al. 2002].

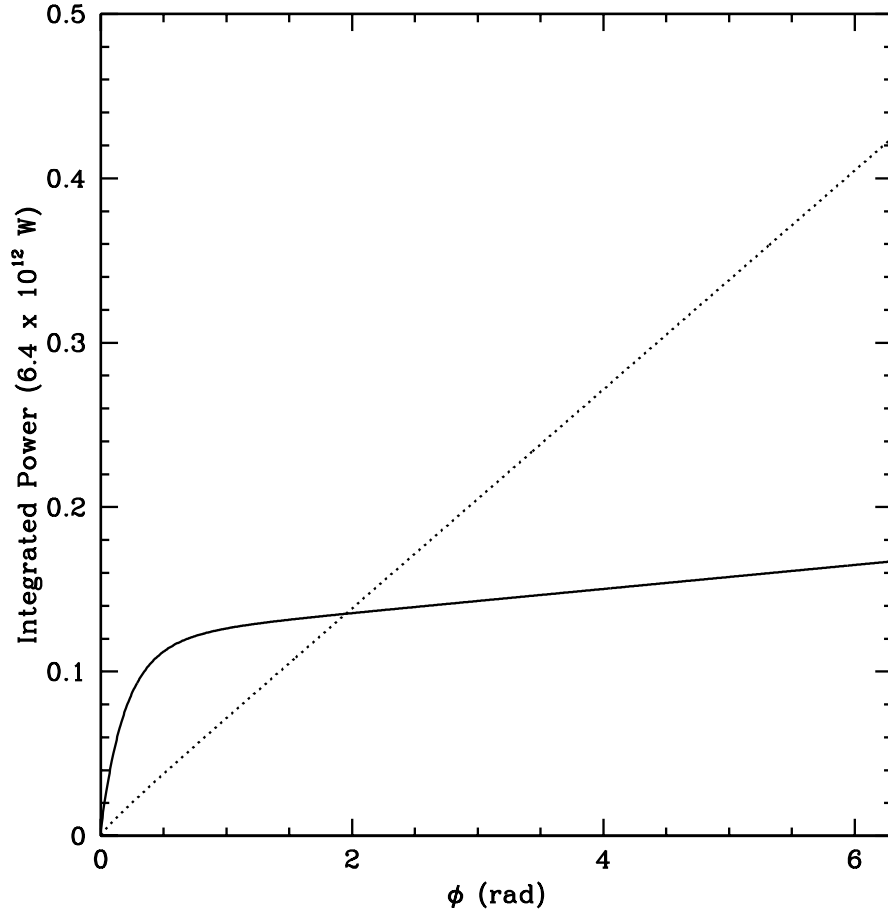


Fig. 2.— Integrated power distributions. The solid line is for the power associated with the Birkeland current. The dotted line corresponds to the power dissipation in the torus.

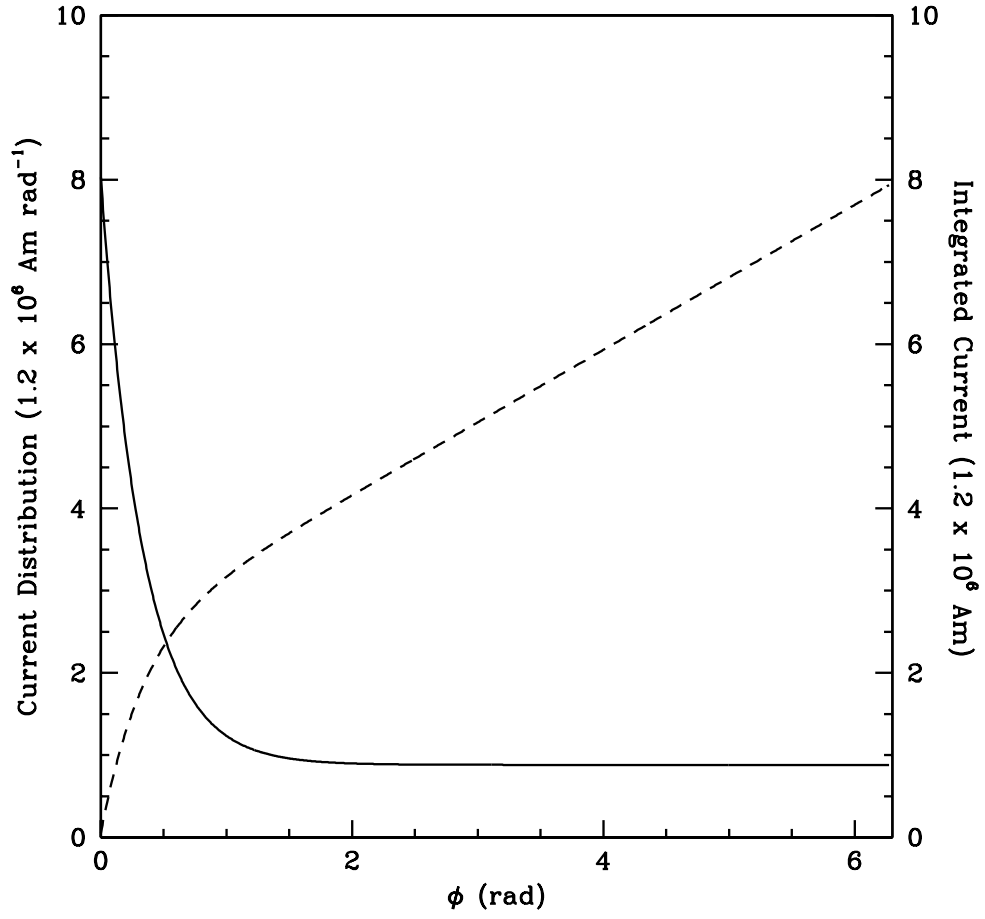


Fig. 3.— Current distribution (solid line, whose scale is on the left-hand side) and integrated current (dashed line, which scales as the right-hand side).